

1-1-2010

## Use of Optical Tweezers to Probe Epithelial Mechanosensation

Andrew Resnick  
Cleveland State University, [a.resnick@csuohio.edu](mailto:a.resnick@csuohio.edu)

Follow this and additional works at: [https://engagedscholarship.csuohio.edu/sciphysics\\_facpub](https://engagedscholarship.csuohio.edu/sciphysics_facpub)

 Part of the [Physics Commons](#)

[How does access to this work benefit you? Let us know!](#)

### *Publisher's Statement*

Copyright 2010 Society of Photo-Optical Instrumentation Engineers. One print or electronic copy may be made for personal use only. Systematic reproduction and distribution, duplication of any material in this paper for a fee or for commercial purposes, or modification of the content of the paper are prohibited. Available from publisher at <http://dx.doi.org/10.1117/1.3316378>.

---

### Original Citation

Resnick, Andrew. "Use of Optical Tweezers to Probe Epithelial Mechanosensation." *Journal of Biomedical Optics* 15 (2010): 15005.

### Repository Citation

Resnick, Andrew, "Use of Optical Tweezers to Probe Epithelial Mechanosensation" (2010). *Physics Faculty Publications*. 39.  
[https://engagedscholarship.csuohio.edu/sciphysics\\_facpub/39](https://engagedscholarship.csuohio.edu/sciphysics_facpub/39)

This Article is brought to you for free and open access by the Physics Department at EngagedScholarship@CSU. It has been accepted for inclusion in Physics Faculty Publications by an authorized administrator of EngagedScholarship@CSU. For more information, please contact [library.es@csuohio.edu](mailto:library.es@csuohio.edu).

# Use of optical tweezers to probe epithelial mechanosensation

**Andrew Resnick**

Cleveland State University  
Department of Physics  
2121 Euclid Avenue  
Cleveland, Ohio 44115

**Abstract.** Cellular mechanosensation mechanisms have been implicated in a variety of disease states. Specifically in renal tubules, the primary cilium and associated mechanosensitive ion channels are hypothesized to play a role in water and salt homeostasis, with relevant disease states including polycystic kidney disease and hypertension. Previous experiments investigating ciliary-mediated cellular mechanosensation have used either fluid flow chambers or micropipetting to elicit a biological response. The interpretation of these experiments in terms of the “ciliary hypothesis” has been difficult due to the spatially distributed nature of the mechanical disturbance—several competing hypotheses regarding possible roles of primary cilium, glycocalyx, microvilli, cell junctions, and actin cytoskeleton exist. I report initial data using optical tweezers to manipulate individual primary cilia in an attempt to elicit a mechanotransduction response—specifically, the release of intracellular calcium. The advantage of using laser tweezers over previous work is that the applied disturbance is highly localized. I find that stimulation of a primary cilium elicits a response, while stimulation of the apical surface membrane does not. These results lend support to the hypothesis that the primary cilium mediates transduction of mechanical strain into a biochemical response in renal epithelia. © 2010 Society of Photo-Optical Instrumentation Engineers. [DOI: 10.1117/1.3316378]

Keywords: laser tweezers; mechanosensation; renal epithelia.

Paper 09297R received Jul. 17, 2009; revised manuscript received Nov. 11, 2009; accepted for publication Dec. 23, 2009; published online Feb. 18, 2010.

## 1 Introduction

Many types of epithelial cells within an organism, upon terminal differentiation, grow a single nonmotile cilium on their free (apical) surface.<sup>1</sup> This organelle, related to the bacterial flagellum, protrudes several microns into the lumen, is encased by the cell membrane, and is composed of a central axoneme containing nine microtubule doublets anchored to the mother centriole. Although its existence and microscopic structure has been known for over four decades, its functions are not well explored and have come under intense investigation with the recent demonstration that bending the cilium induces a release of intracellular calcium.<sup>2</sup> The physiological role of the primary cilium in humans is inferred by experiments linking defects in the cilium and its cellular anchor, the basal body, to several human pathophysiological phenotypes, including Kartagener syndrome,<sup>3</sup> polycystic kidney disease,<sup>4</sup> nephronophthisis,<sup>5</sup> Bardet-Biedl syndrome,<sup>6</sup> and Meckel-Gruber syndrome.<sup>7</sup>

Epithelial tissue provides a functional barrier between “inside” and “outside.” Often just one cell layer thick, epithelial layers are distinguished from other types of tissue due to directed transport of solutes (salts, glucose, etc.) through the

monolayer, which is accomplished by coordinated action of many apical and basolateral membrane transporter proteins.<sup>8</sup> The study of epithelial tissue can be used to gain understanding of the regulatory systems within an organism—for example, total body salt and water content as regulated by the kidney.<sup>9</sup> Mechanosensation, in the context of renal epithelial tissue, refers to the hypothesis that homeostatic mechanisms can regulate total body content of a substance by measuring both concentration (ligand-receptor binding) and volumetric flow rate (possibly by fluid flow induced shear stress).<sup>10</sup>

A complete model of ciliary-mediated mechanosensation and downstream mechanotransduction signaling events in the collecting duct has not yet been developed.<sup>11</sup> The initial event is taken to be the opening of a mechanosensitive ion channel [e.g., polycystin-2 (Ref. 12), transient receptor potential vanilloid (TRPV)-4 (Ref. 13)] in response to ciliary bending, which allows a small number of extracellular  $\text{Ca}^{++}$  ions into the cytosol. This local increase in  $\text{Ca}^{++}$  concentration in turn may open ryanodine receptors (shown in Madin-Darby canine kidney (MDCK) cells<sup>12</sup>), 1,4,5-triphosphate (IP3)-sensitive  $\text{Ca}^{++}$  receptors (shown in pancreatic acinar cells<sup>14</sup>), or perhaps other mechanisms,<sup>15</sup> with a resultant release of large amounts of  $\text{Ca}^{++}$  (calcium-mediated calcium release) into the cytosol. Many regulatory processes are mediated by  $\text{Ca}^{++}$ , including vertebrate left-right asymmetry,<sup>16</sup> cellular growth

Address all correspondence to: Andrew Resnick, Cleveland State University, Department of Physics, 2121 Euclid Avenue, Cleveland, Ohio 44115. Tel: 216-687-2437; E-mail a.resnick@csuohio.edu

and apoptosis,<sup>17</sup> and G-protein-coupled signaling pathways.<sup>18</sup> The cytosolic calcium is then resequenced within the endoplasmic reticulum (ER), and the cycle may begin again upon restimulation of the primary cilium.

## 2 Relevant Previous Work

Several different types of observations indicate that the primary cilium of renal and other epithelial cells can transduce an externally applied mechanical signal to an intracellular signaling pathway.<sup>10,12,19–21</sup> In most previously published experiments,<sup>22–25</sup> the mechanical stimulation was acute steady shear stress applied in the form of forced fluid flow over a confluent monolayer of epithelial cells. Cellular readouts under these conditions were increases in cytosolic  $\text{Ca}^{2+}$  and decreases in stimulated cyclic adenosine monophosphate (cAMP) levels. In other, more recent experiments,<sup>10,26,27</sup> gentler stresses in the form of orbital shaking were applied overnight to epithelial monolayers. In one experiment using shaking,<sup>26</sup> trafficking of the angiotensin receptor type 1 to the apical surface was enhanced. This, combined with the results of another experiment showing that cilia-mediated flow sensing modulates transepithelial sodium flux,<sup>10</sup> suggests the possibility that ciliary mechanosensation plays a role in flow-dependent enhancement of proximal tubular salt and fluid reabsorption. Last, in another experiment, ciliary mechanosensation by mild shaking affected retention of the transcription factor signal transducers and activators of transcription protein 6 (STAT6) in the cilium and prevention of translocation to the nucleus,<sup>27</sup> thus suggesting, together with other data, that the cilium serves as sensor for orienting cell division along the tubular axis.<sup>28</sup>

Even so, experiments have yet to unequivocally demonstrate an essential role of the primary cilium in mechanosensation. While the biological sequelae have been carefully studied, the initial mechanical stimulation has received much less attention. The question of the role of the primary cilium in transducing a biological response to physiologically relevant mechanical stimulation currently remains open, with several alternative pathways proposed.<sup>29,30</sup> Fluid flow experiments, by their nature, apply a shear stress over the entire apical surface of the cells, thus applying a force to (for example) the actin microvilli brush border,<sup>31</sup> the glycocalyx,<sup>32</sup> and the apical membrane, which is mechanically coupled to the cytoskeleton.<sup>33</sup> Additional questions regarding the appropriate magnitude and dynamics of the stimulation also exist. For example, there is no reason to assume that an applied steady stress will produce the same downstream signaling events as an applied unsteady stress. Within the kidney, the flow is clearly unsteady,<sup>34</sup> while experimental conditions apply steady stimulation. A few previous experiments<sup>10,22,35</sup> appear to show that the force-response curve is not graded (i.e., the mechanotransduction pathway is either activated or not), but others may show a graded response.<sup>2</sup>

## 3 Aim of the Study

A first attempt at disentangling the various problems of experimental interpretation is reported here. An experiment was performed to apply a highly localized disturbance directly to an individual primary cilium. Laser tweezers<sup>36</sup> were used to bring a micrometer-sized object directly into contact with a

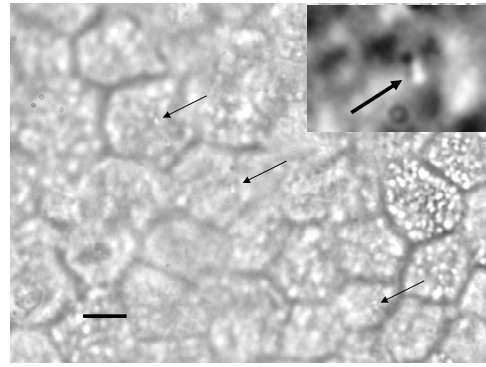


**Fig. 1** *En face* view of terminally differentiated mCCD monolayer. Scale bar is 5 microns. Arrows indicate primary cilia, which grow perpendicular to the cell surface. Typically, between 50% to 80% of cultured cells contain a primary cilium. Inset is a magnified and contrast-enhanced section showing the middle cilium.

primary cilium. The time-varying concentration of cytosolic  $\text{Ca}^{++}$  was used as a cellular readout to indicate whether a physiologically relevant response has occurred as a way to directly connect this work with previous reports. Additional work was performed to demonstrate that a primary cilium could be manipulated directly by the tweezer beam. The results presented here represent an initial study to localize an applied force to the primary cilium as a way to clarify its putative role in the mechanosensitive processes. The work here also provides justification to further develop the methodology and quantitatively study the effects of magnitude and dynamics in mechanosensation and mechanotransduction.

## 4 Methods

### 4.1 Cell Culture

Experiments were carried out with a mouse cell line derived from the cortical collecting duct [mCCD 1296 (d)] of a heterozygous offspring of the Immortomouse (Charles River Laboratories, Wilmington, Massachusetts). The Immortomouse carries as transgene a temperature-sensitive SV40 large T antigen under the control of an interferon- $\gamma$  response element. Cells were maintained on collagen-coated Millicell-CM inserts (Millipore Corp, Billerica, Massachusetts) to promote a polarized epithelial phenotype. Cells were grown to confluence at 33 °C, 5%  $\text{CO}_2$  and then maintained at 37 °C, 5%  $\text{CO}_2$  to enhance differentiation. The growth medium consisted of the following (final concentrations): Dulbecco's Modified Eagle Medium (DMEM) w/o glucose and Ham's F12 at a 1:1 ratio, 5 mM glucose, 5  $\mu\text{g}/\text{ml}$  transferrin, 5  $\mu\text{g}/\text{ml}$  insulin, 10 ng/ml epithelial growth factor (EGF), 4  $\mu\text{g}/\text{ml}$  dexamethasone, 15 mM 4-(2-hydroxyethyl)-1-piperazineethanesulfonic acid (HEPES), 0.06%  $\text{NaHCO}_3$ , 2 mM L-glutamine, 10 ng/ml mouse interferon- $\gamma$ , 50  $\mu\text{M}$  ascorbic acid 2-phosphate, 20 nM selenium, 5% fetal bovine serum (FBS). For differentiation, FBS, insulin, and interferon- $\gamma$  were omitted from the apical medium and insulin, EGF, and interferon- $\gamma$  from the basal medium. The cells developed cilia and became fully differentiated (from transepithelial electrophysiology; see Ref. 10) after 2 weeks of culture in differentiation conditions.

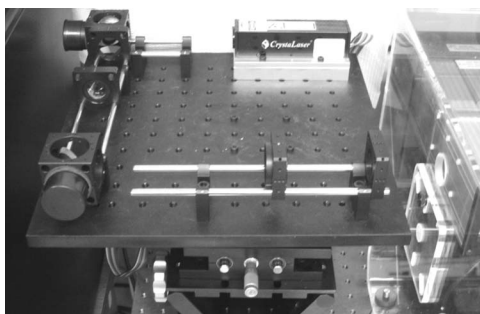


**Fig. 2** Laser tweezer apparatus. The laser tweezer is coupled into the fluorescence turret via a side-look mirror and is located outside the incubation chamber.

An *en face* image of the cultured cells after complete differentiation is shown in Fig. 1.

#### 4.2 Calcium Fura-2 Protocol

The protocol follows that from Nauli.<sup>12</sup> A stock solution of 1 mM Fura-2AM was first prepared, consisting of 1 mg Fura-2AM into 1 mL dispersant solution, consisting of 20 wt% Pluronic F-127 in 80 wt% dimethyl sulfoxide (DMSO). The cells were incubated with the stock solution diluted down to 5  $\mu$ M at 37 °C for 30 min. The monolayer was washed three times with DMEM to remove excess Fura-2AM and the insert placed into a 60-mm culture dish with DMEM (phenol red indicator omitted, 1 mM probenecid added), which was then placed within the microscope incubation chamber. The illuminator source was a Lambda DG-4 switchable source that alternately illuminated the cells with 340-nm and 380-nm light, corresponding to the different absorption peaks of Ca<sup>++</sup>-free and Ca<sup>++</sup>-bound states of Fura-2. A dichroic filter cube (Chroma filter set 71000A) within the microscope was used to illuminate and detect the Fura-2.

#### 4.3 Optical Tweezers

See Fig. 2. The source was a Crystalaser IRCL-0.5-W-1064, a diode-pumped Nd:YAG continuous-wave single-mode laser providing 0.5-W optical power from a 10-W electrical power supply. The optical tweezer breadboard layout was constructed using Linos Microbench optomechanical mounts. Achromatic doublets were used for the beam expansion. The first lens has a 10-mm focal length, while the second has a 200-mm focal length. Both lenses were antireflection coated for 1064 nm. The focal lengths were chosen simply for convenience: the distance between the entrance port of the microscope and the objective lens is 140 mm, and the laser beam was expanded a factor of about 6 $\times$  to fill the aperture. The objective lens used was a Leica 63 $\times$  NA 0.9 U-V-I HCX long working distance plan apochromat dipping objective with a 2.2-mm working distance. The tweezer couples into the microscope through an existing lateral port. A side-looking 1064-nm dichroic mirror (Chroma) mounted within the fluorescence turret provides the ability to perform normal transillumination microscope viewing while the tweezers are operating. A KG-1 IR cutoff filter (Newport) was permanently installed within the imaging path above the fluorescence turret to attenuate the Nd:YAG beam during alignment and trapping

operations. The small amount of leakage from the backscattered tweezer light through the two dichroic filters allows observation of the tweezer spot by a camera during alignment and operation. The trapping beam was used to apply a force to individual cells by moving the microscope stage; the trapping beam does not move.

#### 4.4 Microscopy

Imaging and manipulations of terminally differentiated epithelial monolayers were carried out using a Leica DM 6000 upright microscope equipped with a heated and CO<sub>2</sub> controlled incubation chamber (Solent Scientific). Calcium imaging was performed using a Princeton Instruments 512 EM-CCD camera and a Sutter Instruments Lambda DG-4 switchable source. Bright-field images and optical trap monitoring was performed by a Point Grey Instruments “Flea” camera. Calcium images were acquired using MetaFluor, and typical exposure times were 300 ms. Image pairs were acquired every 10 s and analyzed using MetaFluor Analyst. Monolayers were found to be viable for up to 4 h, “viability” defined here as a Ca<sup>++</sup> response to adenosine triphosphate (ATP) stimulation, and in addition, maintenance of transepithelial resistance.

#### 4.5 Microscope Sample Stage

Because of the nature of the experiments presented here, I present some information regarding the sample stage. The motion in *z* (along the optical axis) was controlled by the Leica microscope, a microstepper motor with a resolution of 0.015  $\mu$ m. A display allows quantitative control of the *z*-stage displacement. Motion in *x* and *y* was accomplished by use of a motorized Prior stage (H101A ProScanII) with a minimum step size of 0.01  $\mu$ m.

#### 4.6 Tweezer Characterization

A complete characterization of the trap stiffness is beyond the scope of this paper. Rather, the relevant information is simply that the force applied to a cilium is within a physiologically relevant range. Two methods were used to assess the maximum applied force: holding a sphere and moving the stage,<sup>37</sup> and holding a sphere in an applied flow via a flow chamber.<sup>36</sup> Polystyrene microspheres suspended in phosphate-buffered saline (PBS) were used. A microsphere was trapped far from a surface, and the sample stage moved at a slowly increasing velocity until the sphere fell out of the trap. The trapping force is then (approximately) given by the Stokes drag force. This method correlated well with the alternative method, holding a sphere stationary in the presence of applied steady flow created by a digitally controlled peristaltic pump (Ismatec REGLO ISM 834). It should be noted that use of long tubes of small diameter connecting the pump to the chamber caused the flow within the flow chamber to be steady rather than rectified. Both measurements indicated the trap strength of a 2- $\mu$ m-diam latex sphere in PBS of approximately 210 pN. This is in the range of forces within a renal tubule,<sup>38</sup> indicating that a trapped sphere can be used to apply a physiologically relevant force to a cilium.

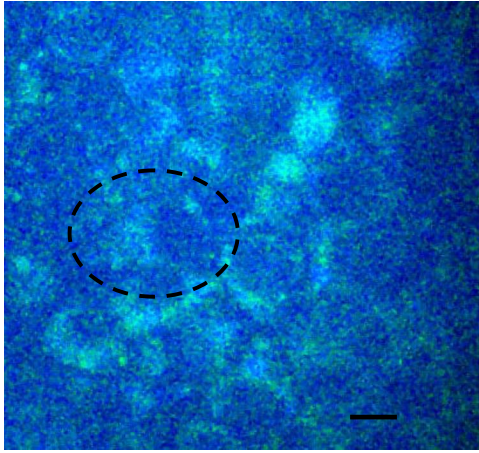


**Fig. 3** Example ratiometric Fura-2 image. This image represents the ratio of two images, one acquired using 340-nm excitation and the other using 380-nm excitation. The circled cell is the one that was manipulated with the laser tweezer. Scale bar is 5 microns.

#### 4.7 Calcium Imaging and Trapping

An example ratiometric image is shown in Fig. 3. With Metafluor running and acquiring images, the filter turret was manually rotated from the Fura-2 cube to the tweezer cube and the illumination changed to bright field.

Observing the trapped particle and monolayer with the Flea camera, the trapped particle was rubbed either against the apical surface or against the primary cilium of a single cell several times before returning the microscope back to calcium imaging configuration. A consequence of this procedure is that a few frames during the time course contain artifacts of the Nd:YAG illumination and are consequently omitted from the presented data. It should be noted that the combination of the dichroic mirror and the KG-1 filter did not completely eliminate the backscattered trapping illumination. This is due to the extreme sensitivity of the CCD array.

#### 4.8 Sample Size

Multiple measurements were performed on multiple monolayers. Each experimental result presented here represents results obtained on four different confluent monolayers (with passage numbers between 42 and 54), each monolayer used up to five times (contingent on monolayer viability), and each daily individual experimental run was performed on three different cells from a single confluent monolayer. This sample size, combined with the clonal nature of the cell line, indicates the results obtained are robust.

## 5 Results

### 5.1 The Tweezers Can Directly Trap a Cilium with Sufficient Force to Move It

There are two ways the optical tweezers can be used to apply a force to a primary cilium. One way is to trap a small object (e.g., microsphere) and, using the object, push against the cilium. A second way is to directly trap the cilium and move the cell, causing a deformation in the cilium to occur. The advantage of the first method is that the trapping force, and thus the force applied to the cilium, can be calculated much

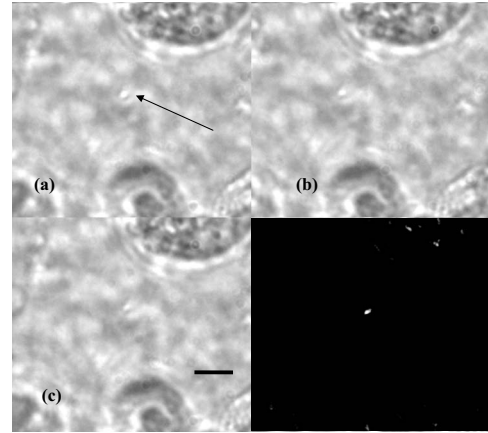


**Fig. 4** Optically trapped cilium. Scale bar is 5 microns. Arrow indicates the cilium. Frame (d) is a subtraction of frame (c) from frame (a) and clearly indicates that the cilium can be moved directly by the optical trap in spite of the submicron dimensions of the cilium.

more accurately. The advantage of the second is that the tweezers apply a force to the cilium without any sort of material contact occurring. The disadvantage of the first method is that downstream signaling effects could be caused by the physical contact between trapped object and cilium rather than the applied stress itself. The disadvantage of the second method is that the applied force is known much less accurately, due to lack of detailed knowledge of the optical properties of the cilium, the high aspect ratio (length/diameter  $\sim 20$ ) of the cilium, and the fact that a cilium is anchored at one end to the cell. Because use of a trapped particle to deform a primary cilium will allow for the possible confounding effects of physical contact, I attempted to directly trap a primary cilium with the optical tweezers and cause the cilium to deform. Given the small diameter of the cilium ( $0.2 \mu\text{m}$ ), it was expected that any trapping force would be small, possibly insufficient to cause ciliary deformation. Example results are shown in Fig. 4.

These images are taken from a video sequence and show that a primary cilium can be stably trapped and held in the trap with sufficient force to allow for significant deformation. Using published data for the mechanical stiffness of the primary cilium,<sup>25</sup> applying the trap to the distal tip of the cilium, and measuring the maximal deflection of the cilium tip from acquired images allowed the deformed cilium to be modeled as a homogeneous cylindrical cantilevered beam<sup>38</sup> and thus estimate the applied force. Using this data, the applied force was estimated to be approximately 1 pN. Based on perfused tubule data,<sup>35</sup> this is not a physiologically relevant force. Consequently, trapped particles were used to apply mechanical disturbances to cilia for the remainder of this study.

### 5.2 Trapping Does Not Damage the Monolayer

It is important to note that confluent monolayers represent a functional entity that is highly sensitive to even small changes in individual constituent cells.<sup>39</sup> Specifically, loss of, or damage to, a single cell is sufficient to render the entire monolayer nonfunctional. Even though the trapping wavelength was chosen to minimize absorption and photodamage,<sup>40</sup> because monolayer integrity is so different from apoptosis of isolated

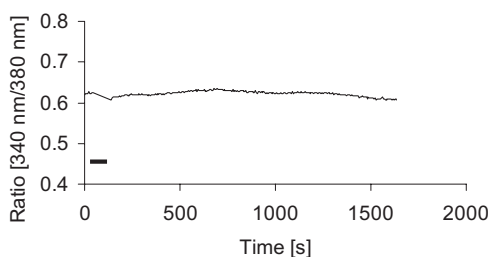


**Fig. 5** Ratiometric Fura-2 trace of a region containing a cell stimulated by the laser tweezer beam. An apical region of a cell, far from the primary cilium, was illuminated by the trapping laser. Scale bar indicates the time of illumination. Ratiometric image acquisition was paused during tweezer stimulation.

cells, it was necessary to determine that the trapping laser did not irreparably damage the monolayer, either directly through photodamage and heating, or indirectly by heating the apical medium. The trapping laser was trained on a single cell and held in place for several minutes, representing a much longer exposure than occurs for trapping and stimulation. The monolayer (still within the culture well) was then placed into a voltometer (World Precision Instruments Endohm chamber), which showed that the transepithelial resistivity remained undisturbed [monolayer resistance was typically 1 to 2  $k\Omega \cdot \text{cm}^2$ ; Ref. 10]. There was evidence that the trapping beam heated the medium, as seen by the appearance of large-scale convective motion, which would bring cellular debris from elsewhere into the field of the view of the camera. However, no flow-induced biological effects were observed (as verified by  $\text{Ca}^+$  ratiometric imaging). The induced flow did not appear to damage the viability of the monolayer either, also verified by transepithelial electrophysiology. Consequently, although the tweezer beam may induce biological effects, the readouts chosen here are not affected.

### 5.3 Applying the Tweezer Directly to the Cell Membrane Does Not Elicit a Calcium Response

Two procedures were performed to ascertain whether application of the tweezer beam would result in the release of intracellular  $\text{Ca}^{++}$ . The trapping beam was applied directly to the apical cell membrane, far from the primary cilium. For one set of experiments, the trap was held steady in one position for a minute. For other experimental runs, the cells were moved in an oscillatory fashion for one minute, keeping the trap far from the primary cilium. The time scale was chosen based on flow-type stimulation, in which the release of intracellular calcium occurs very rapidly upon onset of flow.<sup>12</sup> An example trace of the measured fluorescence ratio is shown in Fig. 5. The graph shows no significant change in the concentration of cytosolic  $\text{Ca}^{++}$  mechanotransduction pathways. This demonstrates that the optical trap, in itself, does not cause the release of intracellular  $\text{Ca}^{++}$ .

### 5.4 Physical Contact of a Trapped Particle Against the Cell Membrane Does Not Elicit a Calcium Response

In another experiment, a trapped particle was pushed into physical contact with the apical surface of a cell (far from a

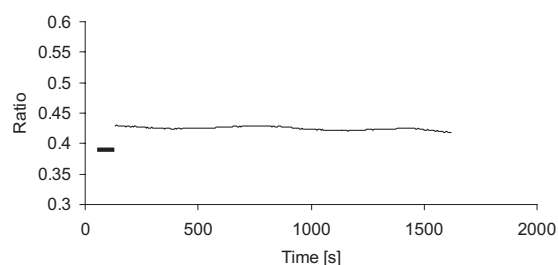


**Fig. 6** Ratiometric Fura-2 trace of a region containing a cell stimulated by a trapped particle. The trace was calculated based on a region of several cells. An apical region of a single cell, far from the primary cilium, was stimulated by a trapped particle for 1 min. Scale bar indicates duration of stimulation. Ratiometric image acquisition commenced upon cessation of stimulation.

cilium). Because the axial intensity gradient is approximately five times less than the radial gradient for an NA 0.9 beam,<sup>41</sup> the estimated maximum downward force exerted on the membrane was 50 pN. The actual force applied was likely substantially lower, corresponding to an observed bead displacement of approximately 1 micron, based on  $z$ -axis displacement of the microscope stage while maintaining the bead in optical focus. This experiment was performed to more closely emulate the micropipetting technique of Praetorius and Spring<sup>2</sup> and Sanderson and Dirksen.<sup>42</sup> The trapped particle was sinusoidally oscillated along the surface for one minute. The results of the Fura-2 images are shown in Fig. 6.

Interestingly, stimulation of the apical surface by physical contact did not induce the release of calcium into the cytosol, indicating that any mechanotransduction apparatus is not likely located indiscriminately along the apical surface. One important and relevant distinction between this result and the contrary result reported by Sanderson et al.<sup>43</sup> is the magnitude of applied force; Sanderson's work reported pushing a micropipette 6  $\mu\text{m}$  into the cell membrane, while the deformation reported here is substantially less.

It should be noted that the null results obtained here and earlier collectively imply that any induced forces caused by motion of the microscope stage are also insufficient to provoke intracellular  $\text{Ca}^{++}$  release.

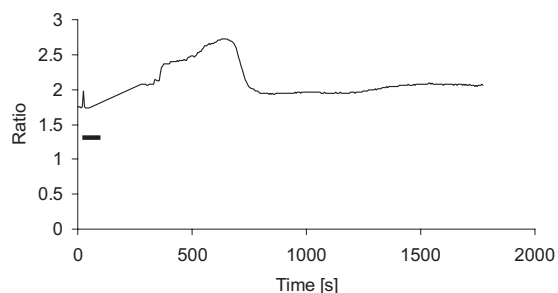


**Fig. 7** Ratiometric Fura-2 trace of a region containing a cell stimulated by a trapped particle. Here, a primary cilium was manipulated as Fig. 7, and the Fura-2 trace was calculated over a region of several cells. Scale bar indicates time and duration of stimulation. The small spike is an artifact of the experimental procedure.

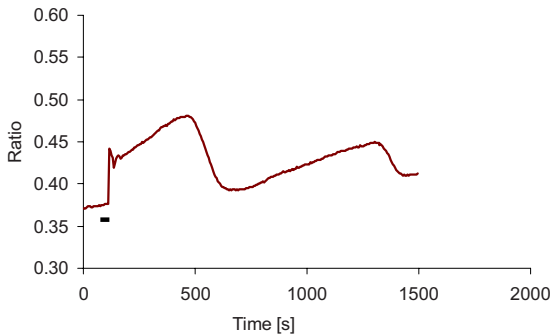


**Fig. 8** Ratiometric Fura-2 trace of a region containing cells stimulated by apical addition of 2 mM ATP. Scale bar indicates time of addition of solution. The small spike is an artifact of the experimental procedure.

### 5.5 Pushing a Trapped Microsphere against the Cilium Correlates with the Release of Intracellular $\text{Ca}^{++}$

Here, a trapped microsphere was brought into contact with the cilium once, with a typical Fura-2 trace shown in Fig. 7. Clearly, contact with the primary cilium did elicit a response. Based on the trap characterization data and the size of the trapped particle,<sup>37</sup> the applied force was not more than 200 pN. The interpretation is that a localized force applied directly to the primary cilium elicited release of intracellular  $\text{Ca}^{++}$ , in agreement with previous reports.<sup>2</sup> This result, taken with the lack of intracellular calcium release when a force is applied elsewhere on the apical surface, implies that the primary cilium is the seat of mechanosensation in renal epithelia.

### 5.6 ATP Applied Apically Did Elicit Intracellular $\text{Ca}^{++}$ Release (Not Due to Flow)

As a final control, ATP was acutely applied to the apical media. This was regularly done as a way to check the overall viability of the monolayer, as ATP is a potent agonist of  $\text{Ca}^{++}$  release. Using a syringe and micropositioner, a small volume (several microliters, representing a sub 0.1% change in apical volume) of ATP in DMEM was added to the apical surface. The final ATP concentration, after addition to the apical surface, was approximately 1 mM, well in excess of the binding constant. The  $\text{Ca}^{++}$  trace (Fig. 8) shows the characteristic response due to the presence of P2-purinergic receptors.<sup>44</sup> It is important to note that this response was not due to flow induced by the addition of agonist; this was verified by adding DMEM alone at the same rate of application (results not shown).

## 6 Discussion

### 6.1 Magnitude of Applied Force

The specific deformation state of the cilium (and resultant elastic strain energy) is highly dependent on the distribution of load along the length as well as the mechanical properties of the cilium. While very little detailed experimentation to measure the physical properties of the cilium has been performed,<sup>38</sup> preliminary results indicate that the cilium can be adequately modeled as a homogeneous slender cantilevered cylinder with a free end and a built-in end, and with a

bending modulus of  $31 \text{ pN} \cdot \mu\text{m}^2$  (Ref. 25). To simplify interpretation of the experimental results presented here, the force was consistently applied as close to the free end of the cilium as possible. Numerical solution of this system has been performed, and preliminary results have been presented elsewhere.<sup>38</sup> Those prior results provided much of the justification for the experimental work presented here.

### 6.2 Stimulation of the Apical Surface

There exists a sizable body of evidence that the molecular origin of mechanosensation may not be related to the primary cilium (see, for example, Refs. 32 and 45). It is important to note that this evidence is predicated on fluid flow stimulation of epithelia—that is, the applied force was distributed over the entire apical surface. If direct stimulation of the apical membrane can induce a release of intracellular  $\text{Ca}^{++}$ , one interpretation would be that mechanosensation is not strictly mediated by the primary cilium, and that mechanosensitive proteins exist indiscriminately on the apical membrane.<sup>33</sup> However, the experimental results indicate that direct stimulation of the apical surface, with or without physical contact with the membrane, does not elicit an intracellular  $\text{Ca}^{++}$  release. These results indicate that in principal cells of the cortical collecting duct, the apical membrane does not participate in mechanotransduction.

### 6.3 Statistical Significance of Results

The various Fura-2 curves were obtained for multiple experiments, performed on multiple cells within multiple confluent monolayers. Thus, the results presented are robust against cell-to-cell variations as well as variations of the amount of Fura-2 dye loaded into the cell. Pharmacological manipulations allowing quantitative conversion of the dual-wavelength ratio to calcium concentration<sup>46</sup> were not performed at the time due to effects of calcium deprivation on the integrity of the monolayer.<sup>47</sup>

### 6.4 Effects of Applying a Localized Disturbance

The major difference between previous reports and the results reported here is the use of a method that applies a highly localized disturbance—the spatial extent of the applied disturbance is on the order of a square micron or less. Consequently, this experimental method does not suffer from any ambiguity about where the applied forces act. The results presented here, taken together, tell a compelling story—it is possible to apply a localized force directly to a primary cilium using laser tweezers, the magnitude of this force can generally exist within a physiologically relevant range, and application of a localized force directly to a primary cilium elicits a physiological response, as previous reports indicate. This report also presents preliminary data that apical force sensing occurs only via the primary cilium, and that the mechanosensitive apparatus is not indiscriminately located on the apical surface. One possible explanation between the null results reported here and positive results reported by other groups is that the actin-integrin force sensing apparatus occurs on the basolateral surface, which can be stimulated when the entire monolayer is subjected to shear stress on the apical surface.

At this time, the apparatus is not able to directly trap a cilium (or bead) while simultaneously performing Fura-2 ra-

tiometric imaging due to both beamlines sharing the fluorescence turret. Consequently, one remaining potential ambiguity is that the cilium-mediated response was obtained by physical contact of a trapped particle onto the cilium, rather than a mechanosensation mechanism. Even so, the data presented here is sufficient to distinguish between cilium-mediated mechanotransduction and alternative hypotheses.

## 7 Conclusion

This study presents evidence that a physiologically relevant mechanical force applied directly to the cilium elicits the release of intracellular  $\text{Ca}^{++}$ , while forces of similar magnitude applied indiscriminately to the apical surface do not. Trapped beads were used to provide the mechanical stimulus.

The importance of this study as compared to previous experiments is that the force was applied locally, rather than indiscriminately over the apical surface. Thus, this study is able to discriminate between alternate hypotheses of mechanosensation, whereas previous studies were not able to. Specifically, the results presented here indicate that the molecular origin of epithelial mechanosensation lies with the primary cilium, and not with, for example, the glycocalyx or brush border.

## 8 Future Work

In the near future, the microscope will be outfitted with a quadrant photodiode (Phresh Photonics SiQu50-M), which will be used to determine the detailed trap characteristics of a directly trapped cilium. This will allow a measurement of the force-response curve, as well as allow *in situ* measurements of the mechanical properties of the primary cilium. Additional work to apply an oscillatory force is also planned. Last, work has begun trying to perform Fura-2 imaging (and fluorescence imaging in general) while concurrently trapping, and this will more definitively spatially and temporally localize the mechanotransduction.

## Acknowledgments

This work was performed under the NIH K25 DK071027 award. Much of this work was performed while the author was at Case Western Reserve University, Department of Physiology and Biophysics. The author would like to thank Ulrich Hopfer and Margaret Finesilver for their patient assistance during the performance of this work.

## References

1. J. R. Davenport and B. K. Yoder, "An incredible decade for the primary cilium: a look at a once-forgotten organelle," *Am. J. Physiol. Renal Physiol.* **289**(6), F1159–F1169 (2005).
2. H. A. Praetorius and K. R. Spring, "Bending the MDCK cell primary cilium increases intracellular calcium," *J. Membr. Biol.* **184**(1), 71–79 (2001).
3. B. Chin, D. Negre, O. Merrot, J. Pham, Y. Tourneur, D. Ressenkoff, M. Jaspers, M. Jorissen, F. L. Cosset, and P. Bouvagnet, "Ciliary beating recovery in deficient human airway epithelial cells after lentivirus *ex vivo* gene therapy," *PLoS Genet.* **5**(3), e1000422 (2009).
4. T. Weimbs, "Polycystic kidney disease and renal injury repair: common pathways, fluid flow, and the function of polycystin-1," *Am. J. Physiol. Renal Physiol.* **293**(5), 1423–1432 (2007).
5. F. Hildebrandt, M. Attanasio, and E. Otto, "Nephronophthisis: disease mechanisms of a ciliopathy," *J. Am. Soc. Nephrol.* **20**(1), 23–35 (2009).
6. N. A. Zaghoul and N. Katsanis, "Mechanistic insights into Bardet-Biedl syndrome, a model ciliopathy," *J. Clin. Invest.* **119**(3), 428–437 (2009).
7. S. A. Cook, G. B. Collin, R. T. Bronson, J. K. Naggert, D. P. Liu, E. C. Akeson, and M. T. Davisson, "A mouse model for Meckel syndrome type 3," *J. Am. Soc. Nephrol.* **20**(4), 753–764 (2009).
8. W. F. Boron, *Medical Physiology*, Saunders, Philadelphia (2003).
9. B. M. Brenner, *The Kidney*, 7th ed., Saunders, Philadelphia (2003).
10. A. Resnick and U. Hopfer, "Force-response considerations in ciliary mechanosensation," *Biophys. J.* **93**(4), 1380–1390 (2007).
11. S. M. Nauli and J. Zhou, "Polycystins and mechanosensation in renal and nodal cilia," *BioEssays* **26**(8), 844–856 (2004).
12. S. M. Nauli, F. J. Alenghat, Y. Luo, E. Williams, P. Vassilev, X. Li, A. E. Elia, W. Lu, E. M. Brown, S. J. Quinn, D. E. Ingber, and J. Zhou, "Polycystins 1 and 2 mediate mechanosensation in the primary cilium of kidney cells," *Nat. Genet.* **33**(2), 129–137 (2003).
13. Y. N. Andrade, J. Fernandes, E. Vazquez, J. M. Fernandez-Fernandez, M. Arniges, T. M. Sanchez, M. Villalon, and M. A. Valverde, "TRPV4 channel is involved in the coupling of fluid viscosity changes to epithelial ciliary activity," *J. Cell Biol.* **168**(6), 869–874 (2005).
14. M. H. Nathanson, A. D. Burgstahler, and M. B. Fallon, "Multistep mechanism of polarized  $\text{Ca}^{2+}$  wave patterns in hepatocytes," *Am. J. Physiol.* **267**(3 Pt 1), G338–G349 (1994).
15. K. Lange and J. Gartzke, "F-actin-based Ca signaling—a critical comparison with the current concept of Ca signaling," *J. Cell Physiol.* **209**(2), 270–287 (2006).
16. A. Langenbacher and J. N. Chen, "Calcium signaling: a common thread in vertebrate left-right axis development," *Dev. Dyn.* **237**(12), 3491–3496 (2008).
17. L. Erb, Z. Liao, C. I. Seye, and G. A. Weisman, "P2 receptors: intracellular signaling," *Pfluegers Arch. Gesamte Physiol. Menschen Tiere* **452**(5), 552–562 (2006).
18. S. Muallem and T. M. Wilkie, "G protein-dependent  $\text{Ca}^{2+}$  signaling complexes in polarized cells," *Cell Calcium* **26**(5), 173–180 (1999).
19. M. Deiner, S. L. Tamm, and S. Tamm, "Mechanical properties of ciliary axonemes and membranes as shown by paddle cilia," *J. Cell Sci.* **104**(4), 1251–1262 (1993).
20. H. A. Praetorius, J. Frokiaer, S. Nielsen, and K. R. Spring, "Bending the primary cilium opens  $\text{Ca}^{2+}$ -sensitive intermediate-conductance  $\text{K}^{+}$  channels in MDCK cells," *J. Membr. Biol.* **191**(3), 193–200 (2003).
21. H. A. Praetorius and K. R. Spring, "Removal of the MDCK cell primary cilium abolishes flow sensing," *J. Membr. Biol.* **191**(1), 69–76 (2003).
22. W. Liu, N. S. Murcia, Y. Duan, S. Weinbaum, B. K. Yoder, E. Schwiebert, and L. M. Satlin, "Mechanoregulation of intracellular  $\text{Ca}^{2+}$  concentration is attenuated in collecting duct of monocilia-impaired orpk mice," *Am. J. Physiol.* **289**(5), F978–F988 (2005).
23. S. M. Nauli, Y. Kawanabe, J. J. Kaminski, W. J. Pearce, D. E. Ingber, and J. Zhou, "Endothelial cilia are fluid shear sensors that regulate calcium signaling and nitric oxide production through polycystin-1," *Circulation* **117**(9), 1161–1171 (2008).
24. L. M. Satlin, S. Sheng, C. B. Woda, and T. R. Kleymann, "Epithelial  $\text{Na}^{+}$  channels are regulated by flow," *Am. J. Physiol.* **280**(6), F1010–F1018 (2001).
25. E. A. Schwartz, M. L. Leonard, R. Bizios, and S. S. Bowser, "Analysis and modeling of the primary cilium bending response to fluid shear," *Am. J. Physiol.* **272**(1 Pt 2), F132–F138 (1997).
26. R. J. Kolb, P. G. Woost, and U. Hopfer, "Membrane trafficking of angiotensin receptor type-1 and mechanochemical signal transduction in proximal tubule cells," *Hypertension* **44**(3), 352–359 (2004).
27. S. H. Low, S. Vasanth, C. H. Larson, S. Mukherjee, N. Sharma, M. T. Kinter, M. E. Kane, T. Obara, and T. Weimbs, "Polycystin-1, STAT6, and P100 function in a pathway that transduces ciliary mechanosensation and is activated in polycystic kidney disease," *Dev. Cell* **10**(1), 57–69 (2006).
28. G. G. Germino, "Linking cilia to Wnts," *Nat. Genet.* **37**(5), 455–457 (2005).
29. Z. Du, Q. Yan, Y. Duan, S. Weinbaum, A. M. Weinstein, and T. Wang, "Axial flow modulates proximal tubule NHE3 and H-ATPase activities by changing microvillus bending moments," *Am. J. Physiol. Renal Physiol.* **290**(2), F289–F296 (2006).
30. Y. Duan, N. Gotoh, Q. Yan, Z. Du, A. M. Weinstein, T. Wang, and S. Weinbaum, "Shear-induced reorganization of renal proximal tubule cell actin cytoskeleton and apical junctional complexes," *Proc. Natl.*

- Acad. Sci. U.S.A.* **105**(32), 11418–11423 (2008).
31. P. Guo, A. M. Weinstein, and S. Weinbaum, “A hydrodynamic mechanosensory hypothesis for brush border microvilli,” *Am. J. Physiol. Renal Physiol.* **279**(4), F698–712 (2000).
  32. J. M. Tarbell and E. E. Ebong, “The endothelial glycocalyx: a mechano-sensor and transducer,” *Sci. Signal* **1**(40), pt8 (2008).
  33. L. Loufrani and D. Henrion, “Role of the cytoskeleton in flow (shear stress)–induced dilation and remodeling in resistance arteries,” *Med. Biol. Eng. Comput.* **46**(5), 451–460 (2008).
  34. J. J. Kang, I. Toma, A. Sipos, F. McCulloch, and J. Peti-Peterdi, “Quantitative imaging of basic functions in renal (patho)physiology,” *Am. J. Physiol. Renal Physiol.* **291**(2), F495–502 (2006).
  35. W. Liu, S. Xu, C. Woda, P. Kim, S. Weinbaum, and L. M. Satlin, “Effect of flow and stretch on the  $[Ca^{2+}]_i$  response of principal and intercalated cells in cortical collecting duct,” *Am. J. Physiol. Renal Physiol.* **285**(5), F998–F1012 (2003).
  36. K. Svoboda and S. M. Block, “Biological applications of optical forces,” *Annu. Rev. Biophys. Biomol. Struct.* **23**, 247–285 (1994).
  37. A. Resnick, “Use of optical tweezers for colloid science,” *J. Colloid Sci.* **262**(1), 55–59 (2003).
  38. A. Resnick and U. Hopfer, “Mechanical stimulation of primary cilia,” *Front. Biosci.* **13**, 1665–1680 (2008).
  39. C. A. Bertrand, D. M. Durand, G. M. Saidel, C. Laboisse, and U. Hopfer, “System for dynamic measurements of membrane capacitance in intact epithelial monolayers,” *Biophys. J.* **75**(6), 2743–2756 (1998).
  40. K. C. Neuman, E. H. Chadd, G. F. Liou, K. Bergman, and S. M. Block, “Characterization of photodamage to escherichia coli in optical traps,” *Biophys. J.* **77**(5), 2856–2863 (1999).
  41. M. Born and E. Wolf, *Principles of Optics*, 7th ed., Cambridge University Press, Cambridge, UK (1999), p. 489.
  42. M. J. Sanderson and E. R. Dirksen, “Mechanosensitivity of cultured ciliated cells from the mammalian respiratory tract—implications for the regulation of mucociliary transport,” *Proc. Natl. Acad. Sci. U.S.A.* **83**(19), 7302–7306 (1986).
  43. M. J. Sanderson, I. Chow, and E. R. Dirksen, “Intercellular communication between ciliated cells in culture,” *Am. J. Physiol.* **254**(1), C63–C74 (1988).
  44. G. R. Dubyak and C. El-Moatassim, “Signal transduction via P2-purinergic receptors for extracellular ATP and other nucleotides,” *Am. J. Physiol.* **265**(3 Pt 1), C577–606 (1993).
  45. Z. Du, Y. Duan, Q. Yan, A. M. Weinstein, S. Weinbaum, and T. Wang, “Mechanosensory function of microvilli of the kidney proximal tubule,” *Proc. Natl. Acad. Sci. U.S.A.* **101**(35), 13068–13073 (2004).
  46. G. Grynkiewicz, M. Poenie, and R. Y. Tsien, “A new generation of  $Ca^{2+}$  indicators with greatly improved fluorescence properties,” *J. Biol. Chem.* **260**(6), 3440–3450 (1985).
  47. J. P. Y. Kao, *A Practical Guide to the Study of Calcium in Living Cells, Methods in Cell Biology*, vol. **40**, p. 176, Academic Press, San Diego (1994).